NASA TN D-181


# TECHNICAL NOTE

## D-181

# INVESTIGATIONS OF CREEP BEHAVIOR OF STRUCTURAL JOINTS UNDER CYCLIC LOADS AND TEMPERATURES

By Leonard Mordfin, Nixon Halsey, and Gary E. Greene

National Bureau of Standards

NATIONAL AERONAUTICS AND SPACE ADMINISTRATION

WASHINGTON

October 1959

NATIONAL AERONAUTICS AND SPACE ADMINISTRATION

TECHNICAL NOTE D-181

# INVESTIGATIONS OF CREEP BEHAVIOR OF STRUCTURAL JOINTS UNDER CYCLIC LOADS AND TEMPERATURES

By Leonard Mordfin, Nixon Halsey, and Gary E. Greene



## SUMMARY

Eighty-two structural joint specimens were tested to evaluate the effects of cyclic loads and cyclic temperatures on creep and rupture. The specimens included riveted joints of 2024-T3 clad aluminum alloy, and riveted and spot-welded joints of 17-7 PH (TH 1050) stainless steel. The results of these tests show a wide variance but indicate certain trends which permit the estimation of the cyclic creep behavior of joints.

An analysis of the effects of stress concentration on the tensile rupture strength of riveted joints is presented in appendix A. This, together with data from several other laboratories, shows that the effects are small for joints fabricated from notch ductile materials and conventional rivets.

## INTRODUCTION

In a previous investigation (ref. 1) at this laboratory a method of estimating the creep behavior of structural joints was developed. This method utilizes the tensile, shear, and bearing properties of the materials of the joints and operates under the principle that concentrations and interactions of stresses in joints may be neglected. Recent work at this and other laboratories, which is reviewed in appendix A, justify this assumption within certain limitations.

It has been shown (ref. 2) that when the shear and bearing creep properties of the materials are not available, estimates of the rupture strength of a joint can be made solely from the tensile creep properties of the joint material.

Both of these analyses were developed from test results which were obtained under constant loads and constant temperatures.

Experimental data on aircraft materials indicate that creep behavior under varying loads and temperatures is often different from that which would be estimated on the basis of creep behavior under constant conditions. Hence, some question exists as to whether the analyses of joints under constant conditions are applicable to conditions of varying load and temperature. A partial answer to this question has been obtained, reference 3, but considerable uncertainty still exists. This problem is pertinent to the design of structures for high-performance aircraft.

The research project described herein was undertaken to study the creep behavior of structural joints under cyclic conditions. This investigation was conducted at the National Bureau of Standards under the sponsorship and with the financial assistance of the National Advisory Committee for Aeronautics.

## SYMBOLS

| | |
|---|---|
| $a$ | fraction of rupture life spent at high load or high temperature |
| $A$ | fraction of each cycle spent at high load or high temperature |
| $b$ | fraction of rupture life spent at low load or low temperature |
| $C_L$ | time ratio for rupture |
| $C_\lambda$ | time ratio for deformation $\delta$ |
| $d$ | creep damage |
| $L$ | rupture life |
| $p$ | length of cycle |
| $P$ | load |
| $\Delta t$ | increment of time |
| $T$ | temperature |
| $w$ | net width at minimum cross section |
| $\alpha$ | fraction of time spent at high load or high temperature in reaching deformation $\delta$ |
| $\delta$ | specified allowable deformation |

| | |
|---|---|
| $\lambda$ | time required to reach deformation $\delta$ |
| $\sigma$ | principal stress |
| $\bar{\tau}$ | octahedral shear stress |

Subscripts:

| | |
|---|---|
| a | high |
| b | low |
| br | bearing |
| c | cyclic |
| i | 1,2,3, . . . to rupture |
| t | total |

## SPECIMENS

The experimental work of this investigation was performed on joints of three different designs, designated as D, Q, and R.

The group D joints were fabricated from 2024-T3 clad aluminum-alloy sheet and 2024-T31 aluminum-alloy rivets. The nominal dimensions of these specimens are shown in figure 1(a). These specimens were fabricated at this laboratory and are essentially identical to the group D joints discussed in reference 1.

The group Q and R joints were fabricated from 17-7 PH precipitation hardening stainless-steel sheet. The 17-7 PH sheet was heat-treated to the TH 1050 condition at the Naval Gun Factory prior to the assembly of the specimens. The group Q joints were spot-welded by The Budd Company. The group R joints were riveted at this laboratory with 1/4-inch high-shear rivets. Dimensions of these two joint designs are given in figures 1(b) and 1(c).

It will be noted from figure 1 that the gage lengths of the specimens included two identical joints in tandem. The extensions of the joints under load were obtained by dividing the extensions of the gage length by two. This quantity is used throughout the report where ever reference is made to the extension of a joint. The time to rupture was, conservatively, the time for the weaker of the two joints. The extensions and rupture times, when obtained in this manner, have statistical advantages

over data obtained from specimens containing a single joint. These statistical advantages are described in reference 4.

## EQUIPMENT AND PROCEDURE

The tests were conducted in a 100,000-pound screw-power beam-and-poise testing machine equipped with automatic load maintainers as described in reference 2. The furnaces were fabricated with transite sheet and infrared heating elements. Temperatures were controlled with potentiometer temperature controllers and variable autotransformers. Extensions were recorded with differential transformers which measured the relative displacement of rods attached to the ends of the gage length of the specimen.

The cycles were controlled by cycle timers and were very nearly rectangular in shape. That is, in the cyclic temperature tests, a fraction of each cycle was spent at a high temperature and the remainder was spent at a lower temperature. Similarly, in the cyclic load tests, a fraction of each cycle was spent at a high load and the remainder was spent at a lower load.

In the cyclic temperature tests, cooling was obtained with a blower which circulated air through the furnace. Heating and cooling were accomplished at rates of 50° to 100° F/min. Temperatures were maintained constant within 2° F and uniform within 4° F at each temperature level in the cyclic temperature tests and throughout the cyclic load tests.

In the cyclic load tests, a solenoid was mounted on the weigh beam of the testing machine and alternately lifted or dropped a predetermined weight. The load maintainers adjusted the load on the specimen to keep the beam balanced. Changes in load were accomplished at rates of about 50 lb/sec. Loads were maintained constant within 70 pounds at each load level in the cyclic load tests and throughout the cyclic temperature tests.

For the cyclic temperature tests, the specimens were preheated one hour at the high temperature without load. The test was then started at the low temperature with the test load. No preheat was used for the cyclic load tests. These tests were started at the test temperature with the low load.

# ANALYSIS

## Creep Rupture

Consider a member exposed to a load $P$ and a temperature $T$ for an increment of time $\Delta t$. Let the creep damage $d$ which results from this exposure be defined as follows:

$$d = \frac{\Delta t}{L}(P,T)$$



The simplest analyses that can be applied to creep rupture under varying conditions are based upon the assumption that creep damage is linearly cumulative. Under this assumption, the creep damage produced during any increment of time is independent of the conditions in any other increment of time. Summing up the creep damage to rupture leads to the life fraction rule,

$$\sum_i \frac{\Delta t_i}{L_i}(P_i, T_i) = 1 \qquad (1)$$

In the general case, however, creep damage is not necessarily linearly cumulative, so equation (1) becomes

$$\sum_i \frac{\Delta t_i}{L_i}(P_i, T_i) = C_L \qquad (2)$$

When $C_L < 1$, it is apparent that the varying conditions of load and temperature have hastened creep rupture compared with that which would have been estimated from equation (1). Similarly, when $C_L > 1$, a delay in creep rupture is indicated.

For perfectly rectangular cycles of load or temperature, equation (2) reduces to

$$L_c\left(\frac{a}{L_a} + \frac{b}{L_b}\right) = C_L \qquad (3)$$

In the tests conducted in this investigation, the times required to change loads or temperatures were small compared with the lengths of the cycles. Equation (3) then becomes

$$L_c\left(\frac{a}{L_a} + \frac{1 - a}{L_b}\right) = C_L \qquad (4)$$

Creep Deformation

Creep damage may also be defined as

$$d = \frac{\Delta t}{\lambda}(P,T)$$



Carrying the same analysis through, the following equation which corresponds to equation (4) is obtained:

$$\lambda_c\left(\frac{\alpha}{\lambda_a} + \frac{1 - \alpha}{\lambda_b}\right) = C_\lambda \qquad (5)$$

The quantities $a$ and $\alpha$ will generally not be equal in a given test because rupture and the specified deformation $\delta$ will usually be attained in different parts of different cycles. Similarly, both of these quantities will generally be different from $A$, which is the fraction of each cycle spent at high load or high temperature.

## DISCUSSION OF RESULTS

Some typical creep curves obtained from this investigation are given in appendix B together with a discussion of the modes of failure obtained.

### Constant Load - Constant Temperature

Tests under constant load and constant temperature were conducted on specimens of each of the three designs. Table 1 gives the test loads, test temperatures, times to rupture, and times required to reach 0.015 inch of creep extension. Creep extension is used in this report rather than total extension to reduce the effects of scatter. Experience has shown that a significant part of the timewise scatter of creep data may be attributed to the scatter of the initial extensions. In table I the results for the group D joints include test data on group D joints from reference 1.

Master curves for rupture and for 0.015 inch of creep extension are given in figure 2 to facilitate the interpolation of these data.

## Cyclic Load - Constant Temperature and Constant Load-Cyclic Temperature

Tests of specimens of each of the three designs were conducted under cyclic load and constant temperature conditions and under constant load and cyclic temperature conditions. The test conditions and the test results are given in tables 2 and 3. The time ratios $C_L$ and $C_\lambda$ were computed from equations (4) and (5), where $L_a$, $L_b$, $\lambda_a$, and $\lambda_b$ were estimated from figure 2. The value of $\lambda_c$ was taken from the extensometer records.



It was desired to compare $C_L$ for joints with $C_L$ for the respective sheet materials of the joints. This was made possible by the use of references 5 and 6. In these reports $C_L$ for 2024-T3 clad aluminum-alloy sheet and for 17-7 PH (TH 1050) stainless-steel sheet is tabulated for a variety of cyclic load and cyclic temperature conditions. These data were interpolated and extrapolated with respect to rupture time, temperature, cycle length p, and cycle fraction A. It was thereby possible, in most cases, to estimate $C_L$ for the sheet materials for the same test conditions as those for which $C_L$ for the joints had been determined. This estimation was facilitated by the knowledge that for a rupture which occurs during the first cycle, $C_L$ must be unity since the specimen did not get to "know" whether it was being tested under constant or cyclic conditions.

A comparison of $C_L$ for the joints with $C_L$ for the materials of the joints is given in figure 3. It is important to realize that the values of $C_L$ for the materials, taken singly, are not accurate, having been determined by questionable interpolation and extrapolation. Nevertheless, the overall picture of the relation between $C_L$ for joints and $C_L$ for materials, which is shown in the figure, is felt to be indicative of the true relation.

Figure 3 also shows that, if $C_L$ for a joint is assumed to be equal to $C_L$ for the material, an error of up to 2:1 may result. An alternative design procedure would be to assume that $C_L$ for joints is always unity. In most cases the two methods would be equally satisfactory (or unsatisfactory); however, figure 3 shows that under certain conditions

$C_L$ for joints is less than 0.5 or greater than 2.0. In view of this it appears that the more desirable design procedure is to let $C_L$ for a joint equal $C_L$ for the material of the joint.

In most structural applications involving aircraft subjected to creep, the limiting design condition is not rupture, but a specified allowable deformation. It is, therefore, desirable that a method of estimating $C_\lambda$ for joints be available. A specified extension of a joint cannot be directly related to a single value of strain in the joint material. Hence it may be most convenient to base the estimation of $C_\lambda$ on the corresponding value of $C_L$. In figure 4 values of $C_\lambda$ are plotted against corresponding values of $C_L$ for the joints listed in tables 2 and 3. Here, too, a 2:1 discrepancy band is observed. As before, it is apparently unwise to assign a constant value of unity to $C_\lambda$ for all applications since the actual value may be less than 0.5 or more than 2.0.



A timewise uncertainty of 2:1 in the design of a joint, while undesirable, is not more serious than the stresswise uncertainties encountered in the design of many structural components. Consider, for example, a joint design problem involving an allowable extension of 0.015 inch in 10 hours. Let the temperature be 400° F for a group D joint, and 800° F for group Q and group R joints. Figure 2 permits the computation of the corresponding loads and also those loads corresponding to a time of 20 hours. From these loads it is readily seen that the timewise uncertainty of 2:1 is equivalent to a stresswise uncertainty of 1.07:1 for the group D joint, 1.04:1 for the group Q joint, and 1.09:1 for the group R joint.

## CONCLUDING REMARKS

The creep test results for joints under cyclic loads and cyclic temperatures show a wide variance. No accurate method is available for estimating the behavior of joints under cyclic creep conditions. In the design of a joint which will be subjected to cyclic creep exposures, it appears best to assume that the time ratic for rupture of the joint is equal to the time ratio for rupture of the material of the joint. Furthermore, the time ratio for a specific allowable creep deformation of the joint may be taken as equal to the time ratio for rupture of the joint. Both of these assumptions may lead to discrepancies of up to 2:1, timewise. Greater discrepancies may result, however, from an arbitrary assumption that the time ratios are equal to unity. For the joints tested in this investigation, timewise discrepancies of 2:1 are equivalent to stresswise discrepancies of less than 1.1:1.

An analysis of the concentrations and interactions of stress in riveted joints is presented in appendix A. This analysis is based on the premise that creep is a function of the octahedral shear stress, and leads to the conclusion that for design purposes the tensile rupture strength of a riveted joint is not affected by the stress concentrations and interactions, provided that the joint is fabricated from a notch ductile material. Experimental data have been reviewed which corroborate this conclusion provided conventional rivets are used. The basic premise from which the analysis is developed is uncertain, however, and until considerably more experimental data are available, this conclusion must be regarded as tentative.

National Bureau of Standards,
Washington, D. C., March 27, 1958.

# APPENDIX A

## EFFECTS OF CONCENTRATION AND INTERACTION OF STRESSES ON TENSILE RUPTURE STRENGTH OF RIVETED JOINTS

Equations (3) and (4) relate the cyclic rupture time $L_c$ to rupture times under constant conditions $L_a$ and $L_b$. In this report, $L_a$ and $L_b$ were determined from actual test data on joints. It is desirable to be able to calculate $L_a$ and $L_b$ from test data on materials; however this calculation is complicated by the biaxial stress concentrations which exist in joints.



The creep behavior of materials under biaxial stresses is not fully understood. Recent work by Voorhees and Freeman, reference 7, suggests that where the biaxial state results from a stress raiser in flat sheet under a uniaxial load, creep is apparently a function of the octahedral shear stress.[1] As creep progresses in the vicinity of a stress raiser, the stress distribution usually changes, but there is some indication that the average initial octahedral shear stress on the minimum cross section can be used as a measure of rupture strength.

The above applies only to that class of materials which might be referred to as "notch ductile." Many engineering materials fall into this class (see, for example, refs. 7 to 11) including 2024-T4 aluminum alloy and 17-7 PH stainless steel. The difference between a notch ductile material and one which is notch sensitive apparently lies in the ability of the material to rapidly relax the peak stresses at the base of the notch and still retain considerable creep strength and ductility (refs. 7 and 8).

To evaluate the effects of stress concentration and of the interaction of tensile and bearing stresses on the tensile rupture strength of a riveted joint, it is first necessary to determine the octahedral shear stresses on the minimum cross section. Consider the three schematic specimens of unit thickness in figure 5. Specimen (a) is a plain strip in tension, specimen (b) is a perforated strip in tension, and specimen (c) is a perforated strip in tension and bearing, similar to part of a multiriveted joint. All three specimens have the same average stress on the minimum cross section $P_t/w$. A width/diameter ratio of 4 is

---

[1] Voorhees and Freeman did their work in terms of the "effective stress," which is merely $3/\sqrt{2}$ times the octahedral shear stress.

selected because some pertinent experimental and analytical data for this case are available (refs. 12 to 14.)

The octahedral shear stress for plane stress is

$$\bar{\tau} = \frac{\sqrt{2}}{3}\sqrt{\sigma_1^2 + \sigma_2^2 - \sigma_1\sigma_2}$$

where $\sigma_1$ and $\sigma_2$ are the principal stresses. For specimen (a) in figure 5, the octahedral shear stress everywhere is

$$\bar{\tau} = \frac{\sqrt{2}}{3}\sigma_1 = 0.471\,\frac{P_t}{w}$$

For specimen (b), figure 5, the octahedral shear stresses across the minimum cross section were calculated from the stress distribution, given by Howland (ref. 12). The stress distribution for specimen (c), figure 5, was obtained by performing the superposition diagrammed in figure 6. The stress distribution for specimen (d), figure 6, is obviously similar to that for specimen (b), figure 5, while that for specimen (e), figure 6, was given by Theocaris (ref. 13). For the calculations, a loading ratio of $P_t/P_{br} = 3$ was used.

The resulting octahedral shear stresses across the minimum cross sections of specimens (a), (b), and (c) of figure 5 are given in figure 7. Although the distributions for the three specimens differ, the average octahedral shear stresses for the three are very close to one another. This is not necessarily true in the case of other types of stress raisers. Hence, on the basis of the analysis, the tensile rupture strength of all three specimens may be expected to be approximately equal, provided that they are fabricated from a notch ductile material.

There is some experimental evidence which supports the analysis. Dukes and Padlog studied the tensile rupture strength of 2024-T3 specimens of types (a) and (b), figure 5. Their data were for two temperatures and for width/diameter ratios of 4, 8, and 16. In a private communication from Mr. J. Padlog, Bell Aircraft Corp., it was learned that the tensile rupture strength of the perforated specimen is equal to that of the plain strip within 5 percent.

In reference 14, Bodine, Carlson, and Manning reported the results of tests on specimens of type (c), figure 5, fabricated from 2024-0 aluminum alloy. These results are plotted in figure 8 together with data

obtained in a private communication from Mr. E. G. Bodine, Battelle Memorial Institute, for plain sheet specimens of the same batch of material. Figure 8 shows that decreasing ratios of $P_t/P_{br}$ tend to reduce rupture strength somewhat but not below the rupture strength of the plain sheet. Reference 14 also includes data for $P_t/P_{br} = 1$, but these specimens failed in bearing, not tension, and therefore do not apply here.

Further experimental corroboration of the analysis, for the case of pin-loaded turbine rotors of Ni-Cr-Mo-V steel, is available in reference 15.

In reference 1 a method was proposed for estimating the rupture strength of joints which fail in tension. This method, which is based upon the rupture properties of the joint material, assumes that the stress concentrations do not affect the time to rupture. The foregoing analysis and experimental evidence indicate that this simplifying assumption is justified. Strictly speaking, this has been demonstrated primarily for models such as specimen (c), figure 5. For realistic multiriveted joints, the octahedral shear stress distribution can be somewhat different from the one calculated. It is known, for example, that the introduction of additional holes reduces stress concentration (ref. 16), while moving a hole away from the center line of a strip increases the stress concentration (ref. 17). Tests of multiriveted joints indicate that these secondary effects are small, however. Tests on three designs of riveted joints fabricated from 2024-T3 aluminum alloy (ref. 1) gave tensile rupture lives which showed no systematic deviation from values calculated by the proposed method.

It was desired to seek additional verification using the 17-7 PH group R joints of this investigation (fig. 1(c)). Several tests were conducted to evaluate the tensile rupture strengths of plain sheet specimens of this material. The results of these rupture tests are given in table 4. Figure 9 compares the tensile rupture strengths of the joints with those of the material. The differences between the two are seen to be significant in this case. The discrepancy may result from the fact that these joints employed high shear rivets, which do not fill the holes as completely as conventional rivets do. Substantial differences have been observed between the behaviors of joints fabricated with rivets which fill the holes and those containing rivets which do not fill the holes.

Apparently the current knowledge of creep under combined stresses and existing experimental data are insufficient to completely solve the problem of the effects of stress concentrations and interactions on the rupture strength of joints. For the present, it is suggested that in the design of riveted joints for creep exposures the recommendations of reference 14 be observed, that is, the loading ratio $P_t/P_{br}$ at the critical cross section be kept at a minimum.

# APPENDIX B

## SUMMARY OF TEST RESULTS

### Initial Extensions

The initial extensions of the joints in creep tests under constant load and constant temperature are given in table 1. These values include both the elastic and "instantaneous" plastic extensions of the joints which were obtained upon the application of the test loads. They do not include the thermal expansions resulting from the heating of the joints to the test temperatures.

### Creep Curves

Some typical creep curves obtained from the joints tested are given in figures 10 and 11. The extensions shown are the sums of the elastic and plastic deformations of the joints, and are plotted against total test time. These data were taken from the actual extension-time records. The curves for the joints tested under cyclic conditions were faired through points representing the initial extension, the extension at the end of each cycle (just before cooling or unloading), and the extension at rupture.

### Mode of Rupture

The group D joints were fabricated from 2024-T3 sheet and 2024-T31 rivets. Master rupture curves for these materials in tension and in shear, respectively, are given in reference 1 which also shows that the critical tension area for these joints is 0.195 square inch, and the shearing area of the rivets is 0.304 square inch. With these areas, and the master rupture curves for the materials and master rupture curves for the joint were calculated (fig. 12). The curve for shear failure of the joint is only approximate since it was prepared for a constant $C = 20$, whereas $C = 17$ would provide a better fit. The value of 20 was used in figure 12 only so that the curves for tensile and shear failure could be compared on the same set of coordinates.

Figure 12 indicates that the two curves intersect at B, 6,600 pounds. This means that for loads greater than 6,600 pounds, tensile failures may be expected, whereas for loads smaller, shear failures may be expected. The slopes of the two curves are so nearly equal that minor variations in the material properties could move the point of intersection several thousand pounds up or down.

The group D joints, studied in reference 1, had a point of intersection slightly below C, 5,500 pounds, whereas the group D joints tested in this investigation exhibit an intersection somewhat above A, 7,300 pounds. Typical failures of group D joints in tension and in shear are shown in figures 13(a) and 13(b).

All of the group Q spot-welded joints failed by tension in the sheet except that one which was tested at the highest load, 22,900 pounds. That specimen failed by shearing the spotwelds (figs. 13(c) and 13(d)).

The group R riveted stainless-steel joints all ruptured by tension in the sheet (fig. 13(e)).

## REFERENCES


1. Mordfin, L., and Legate, A. C.: Creep Behavior of Structural Joints of Aircraft Materials under Constant Loads and Temperatures. NACA TN 3842, 1957.

2. Mordfin, L.: Creep and Creep-Rupture Characteristics of Some Riveted and Spot-Welded Lap Joints of Aircraft Materials. NACA TN 3412, 1955.

3. Mordfin, L., Greene, G. E., Halsey, N., Harwell, R. H. Jr., and Bloss, R. L.: Creep and Static Strengths of Large Bolted Joints of Forged Aluminum Alloys under Various Temperature Conditions. IAS preprint 779, 1958.

4. Youden, W. J.: Statistics and Planning Tests at Elevated Temperatures. Proc. SESA, Vol. XI, No. 2, 1954.

5. Guarnieri, G. J.: Intermittent Stressing and Heating Tests of Aircraft Structural Metals. WADC TR 53-24, pt. 1, May 1954; pt. 2, Sept. 1954; pt. 3, Jan. 1956.

6. Salvaggi, J.: Intermittent Stressing and Heating Tests of Aircraft Structural Metals. WADC TR 53-24, pt. 4, May 1957.

7. Voorhees, H. R., and Freeman, J. W.: Notch Sensitivity of Heat-Resistant Alloys at Elevated Temperatures. WADC TR 54-175, pt. 1, Aug. 1954; pt 2, Jan. 1956; pt. 3, Sept. 1956.

8. Voorhees, H. R., and Freeman, J. W.: Notch Sensitivity of Aircraft Structural and Engine Alloys. WADC TR 57-58, pt. 1, May 1957.

9. Dillon, O. W.: Exploratory Creep Rupture of Aluminum Alloys of Elevated Temperature. Tech. Rep. No. 1. Contract No. Nonr 266(34), Office of Naval Res. and Columbia Univ., Mar. 1957.

10. Carlson, R. L., MacDonald, R. J., and Simmons, W. F.: Factors Influencing the Notch-Rupture Strength of Heat-Resistant Alloys at Elevated Temperatures. Trans. ASME, vol. 78, no. 2, Feb. 1956, pp. 349-358.

11. Sessler, J. G., and Brown, W. F., Jr.: Notch and Smooth Bar Stress-Rupture Characteristics of Several Heat-Resistant Alloys in the Temperature Range Between 600 and 1000 F. Proc. ASTM, vol. 56, 1956, pp. 738-752.

12. Howland, R. C. J.: On the Stresses in the Neighborhood of a Circular Hole in a Strip Under Tension. Phil. Trans. Roy. Soc. (London), ser. A, vol. 229, Jan. 1930, pp. 49-86.

13. Theocaris, P. S.: The Stress Distribution in a Strip Loaded in Tension by Means of a Central Pin. Jour. Appl. Mech., vol. 23, no. 1, Mar 1956, pp. 85-90.

14. Bodine, E. G., Carlson, R. L., and Manning, G. K.: Creep Deformation Patterns of Joints Under Bearing and Tensile Loads. NACA TN 4138, 1957.

15. Conrad, J. D., and Mochel, N. L.: Operating Experiences with High-Temperature Steam-Turbine Rotors and Design Improvements in Rotor-Blade Fastening. Trans. ASME, vol. 80, no. 6, Aug. 1958, pp. 1210-1223.

16. Atsumi, A.: On the Stresses in a Strip Under Tension and Containing Two Equal Circular Holes Placed Longitudinally. Jour. Appl. Mech., vol. 23, no. 4, Dec. 1956, pp. 555-562.

17. Ling, C. B.: Stresses in a Perforated Strip. Jour. Appl. Mech., vol. 24, no. 3, Sept. 1957, pp. 365-375.

TABLE I

CONSTANT TEMPERATURE, CONSTANT LOAD TESTS

| Temperature, °F | Load, lb | Initial extension, in. | Time to reach, hr | |
|---|---|---|---|---|
| | | | 0.015 in. creep | Rupture |
| Group D joints | | | | |
| 300 | 11,200 | 0.051 | (a) | 0.07 |
| | 9,250 | .025 | 31. | 31.4 |
| 400 | 7,700 | .018 | 1.2 | 1.6 |
| | 7,300 | .020 | (a) | .70 |
| | 6,600 | [b] .016 | [b] 3.9 | [b] 5.2 |
| | 5,500 | .012 | 15. | 32.8 |
| 500 | 4,500 | .016 | .43 | .60 |
| | 3,500 | .010 | [c] 3.7 | (d) |
| | 2,500 | .006 | [c] 8.7 | (d) |
| | 2,000 | .005 | 33. | 94.0 |
| Group Q joints | | | | |
| 700 | 22,900 | 0.039 | 0.8 | 1.2 |
| 800 | 18,500 | .027 | .45 | 1.0 |
| | 16,400 | .018 | 2.0 | 8.4 |
| | 15,400 | .017 | 3.1 | 21.9 |
| 900 | 12,000 | .013 | .4 | 2.1 |
| | 10,200 | .010 | 1.9 | 11.2 |
| | 8,700 | .006 | 5.4 | 68.4 |
| Group R joints | | | | |
| 700 | 20,500 | 0.045 | 0.6 | 1.3 |
| | 19,000 | .036 | 2.2 | 5.7 |
| | 18,400 | .034 | 2.3 | 8.7 |
| | 16,500 | .033 | 18.8 | (d) |
| 800 | 17,400 | .036 | .15 | .3 |
| | 14,500 | .024 | 1.0 | 8.2 |
| | 14,200 | .024 | .9 | 5.6 |
| | 13,200 | .025 | 3.2 | 19.2 |
| 900 | 11,300 | .026 | .2 | 1.2 |
| | 8,900 | .018 | 1.0 | 8.0 |
| | 8,000 | .016 | 2.0 | 12.9 |
| | 6,300 | .007 | 6.8 | (d) |

[a]Ruptured before reaching this deformation.

[b]Average of three tests.

[c]By extrapolation.

[d]Test discontinued before rupture.

TABLE 2

CYCLIC TEMPERATURE TESTS

| Specimen | Load, lb | Temperature cycle | | | | 0.015 in. creep | | | Rupture | | |
|---|---|---|---|---|---|---|---|---|---|---|---|
| | | A | $T_a$, °F | $T_b$, °F | p, hr | $\lambda$, hr | $\alpha$ | $C_\lambda$ | L, hr | a | $C_L$ |
| Group D joints | | | | | | | | | | | |
| 6D | 6,600 | 0.47 | 400 | 75 | 2 | 9.2 | 0.43 | 1.0 | 9.9 | 0.47 | 0.9 |
| 1D | 6,000 | .46 | 400 | -do- | -do- | 19.3 | .44 | 1.1 | 35.5 | .45 | 1.1 |
| [a]3D-2D | 5,400 | .49 | 400 | -do- | -do- | 47.9 | .49 | 1.3 | 71.4 | .49 | .8 |
| [a]31D-5D | 9,800 | .50 | 300 | -do- | -do- | 5.8 | .46 | .6 | 26.0 | .50 | 1.1 |
| 7D | 3,000 | .44 | 500 | -do- | -do- | 9.9 | .44 | .8 | 11.5 | .43 | 1.0 |
| 8D | 6,600 | .40 | 400 | 200 | -do- | 9.3 | .38 | .9 | 9.5 | .39 | .7 |
| 9D | --do- | .42 | -do- | 300 | -do- | 9.1 | .38 | .9 | 9.6 | .41 | .8 |
| 13D | --do- | .48 | -do- | 75 | 4 | 11.6 | .46 | 1.4 | 18.5 | .44 | 1.6 |
| 15D | --do- | .53 | -do- | -do- | 1 | 3.6 | .47 | .4 | 3.7 | .49 | .3 |
| 12D | --do- | .21 | -do- | -do- | 2 | 23.7 | .20 | 1.2 | 37.9 | .20 | 1.5 |
| [a]32D-11D | --do- | .69 | -do- | -do- | 2 | 7.0 | .66 | 1.2 | 8.2 | .67 | 1.1 |
| 16D | --do- | .17 | -do- | -do- | 1 | 9.8 | .15 | .4 | 9.8 | .15 | .3 |
| Group Q joints | | | | | | | | | | | |
| 60Q | 16,400 | 0.51 | 800 | 75 | 2 | 3.1 | 0.35 | 0.5 | 21.1 | 0.48 | 1.2 |
| [a]63Q-64Q | 15,400 | .50 | 800 | -do- | -do- | 4.4 | .42 | .6 | 24.6 | .48 | .6 |
| 91Q | 14,400 | .49 | 800 | -do- | -do- | 17.5 | .49 | .9 | 173.2 | .49 | 1.9 |
| 61Q | 12,000 | 52 | 900 | -do- | -do- | 1.4 | .29 | 1.0 | 3.5 | .51 | .9 |
| [a]54Q-62Q | 10,200 | .50 | 900 | -do- | -do- | 3.4 | .38 | .7 | 20.6 | .46 | .8 |
| Group R joints | | | | | | | | | | | |
| 50R | 19,000 | 0.50 | 700 | 75 | 2 | 6.1 | 0.49 | 1.4 | 15.4 | 0.50 | 1.6 |
| 49R | 18,400 | .52 | 700 | -do- | -do- | 6.0 | .50 | .9 | 23.2 | .50 | 1.4 |
| [a]43R-44R | 14,200 | .49 | 800 | -do- | -do- | 3.6 | .44 | 1.3 | 11.7 | .49 | .9 |
| 46R | 13,200 | .50 | 800 | -do- | -do- | 6.1 | .49 | 1.2 | 32.0 | .50 | 1.0 |
| 90R | 11,300 | .48 | 900 | -do- | -do- | 1.6 | .38 | 3.0 | 3.4 | .35 | 1.0 |
| 47R | 8,900 | .50 | 900 | -do- | -do- | 3.8 | .47 | 1.8 | 29.3 | .48 | 1.9 |
| 89R | 8,000 | .48 | 900 | -do- | -do- | 7.7 | .48 | 1.8 | (b) | (b) | (b) |

[a]Average results of two tests.

[b]Test discontinued before rupture.

TABLE 3

CYCLIC LOAD TESTS

| Specimen | Temperature, °F | Load cycle | | | | 0.015 in. creep | | | Rupture | | |
|---|---|---|---|---|---|---|---|---|---|---|---|
| | | A | $P_a$, lb | $P_b$, lb | p, hr | $\lambda$, hr | $\alpha$ | $C_\lambda$ | L, hr | a | $C_L$ |
| Group D joints | | | | | | | | | | | |
| 22D | 400 | 0.50 | 7,250 | 940 | 2 | 5.9 | 0.49 | 1.7 | 7.2 | 0.44 | 1.9 |
| 17D | 400 | .48 | 6,600 | -do-- | -do- | 7.5 | .45 | .9 | 13.1 | .44 | 1.1 |
| [a]29D-21D | 400 | .50 | 5,070 | -do-- | -do- | 50.2 | .50 | .6 | 53.1 | .49 | .4 |
| 18D | 300 | .48 | 9,800 | -do-- | -do- | (b) | ---- | --- | 39.1 | .47 | 1.6 |
| [a]19D-25D | 500 | .49 | 2,900 | -do-- | -do- | 13.5 | .47 | .9 | 18.6 | .48 | 1.4 |
| 23D | 400 | .49 | 6,600 | 3,000 | -do- | 7.3 | .44 | .8 | 8.0 | .49 | .8 |
| 20D | --do--- | .45 | --do-- | 5,100 | -do- | 3.5 | .40 | .4 | 3.6 | .42 | .3 |
| 24D | --do--- | .50 | --do-- | 940 | 4 | 6.8 | .41 | .7 | 7.1 | .44 | .6 |
| [a]27D-26D | --do--- | .27 | --do-- | -do-- | 2 | 9.8 | .24 | .6 | 10.7 | .24 | .5 |
| 28D | --do--- | .70 | --do-- | -do-- | 2 | 5.3 | .68 | .9 | 5.4 | .69 | .7 |
| 30D | --do--- | .34 | --do-- | -do-- | 1 | 6.8 | .34 | .6 | 7.7 | .34 | .5 |
| Group Q joints | | | | | | | | | | | |
| 83Q | 800 | 0.56 | 17,400 | 1,000 | 2 | 3.3 | 0.49 | 1.8 | 13.6 | 0.56 | 2.6 |
| 77Q | 800 | .53 | 16,400 | -do-- | -do- | 5.3 | .43 | 1.1 | 23.1 | .53 | 1.5 |
| 84Q | 800 | .49 | 16,000 | -do-- | -do- | 5.7 | .49 | 1.6 | 46.0 | .49 | 1.8 |
| 80Q | 800 | .51 | 15,400 | -do-- | -do- | 8.0 | .50 | 1.3 | 107.3 | .51 | 2.5 |
| 75Q | 900 | .50 | 12,000 | -do-- | -do- | 1.5 | .33 | 1.2 | 5.8 | .50 | 1.4 |
| 78Q | 900 | .47 | 10,200 | -do-- | -do- | 3.7 | .46 | .9 | 26. | .47 | 1.1 |
| 85Q | 900 | .50 | 9,500 | -do-- | -do- | (c) | (c) | (c) | 48. | .50 | 1.0 |
| 82Q | 900 | .50 | 8,700 | -do-- | -do- | 19.6 | .49 | 1.8 | 202. | .50 | 1.5 |
| Group R joints | | | | | | | | | | | |
| 72R | 700 | 0.51 | 20,000 | 1,000 | 2 | 2.1 | 0.48 | 1.1 | 9.4 | 0.51 | 2.4 |
| 73R | 700 | .56 | 19,000 | -do-- | -do- | 3.3 | .39 | .6 | 7.0 | .56 | .8 |
| 74R | 800 | .58 | 15,300 | -do-- | -do- | 1.9 | .47 | 1.5 | 7.3 | .58 | 1.8 |
| 70R | 800 | .51 | 14,500 | -do-- | -do- | 2.0 | .50 | 1.0 | 8.0 | .51 | .8 |
| 71R | 800 | .50 | 14,200 | -do-- | -do- | 3.7 | .46 | 1.4 | 35.8 | .50 | 2.6 |
| 76R | 800 | .50 | 13,200 | -do-- | -do- | 10.0 | .50 | 2.0 | 73.2 | .50 | 2.4 |
| 69R | 900 | .50 | 8,900 | -do-- | -do- | 1.9 | .47 | .9 | 15.7 | .50 | 1.1 |
| 86R | 900 | .50 | 8,000 | -do-- | -do- | 9.8 | .49 | 2.4 | 125.1 | .50 | 4.4 |

[a]Average results of two tests.

[b]Ruptured after 0.011 in. creep.

[c]Extensometer did not operate properly.

TABLE 4

TENSILE RUPTURE TESTS OF 17-7 PH(TH 1050)

STAINLESS STEEL

| Temperature, °F | Stress, lb/in.$^2$ | Time to rupture, hr |
|---|---|---|
| 700 | 140,000 | 0.8 |
| 700 | 140,000 | 16.1 |
| 700 | 140,000 | 20.0 |
| 800 | 106,000 | 8.7 |
| 800 | 106,000 | 10.6 |
| 900 | 66,000 | 12.6 |
| 900 | 66,000 | 31.3 |

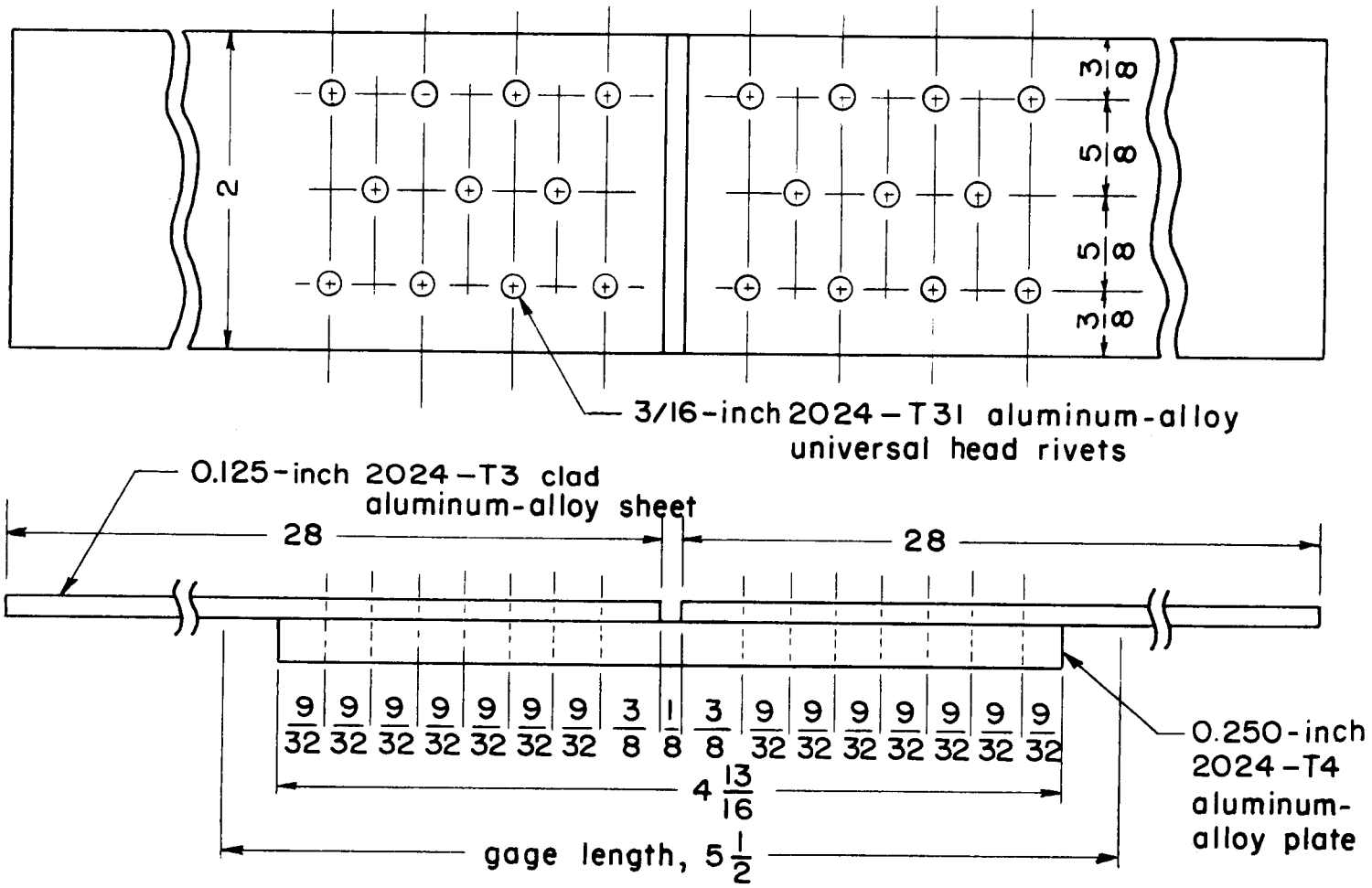


(a) Group D.

Figure 1.- Dimensions of specimens in inches.

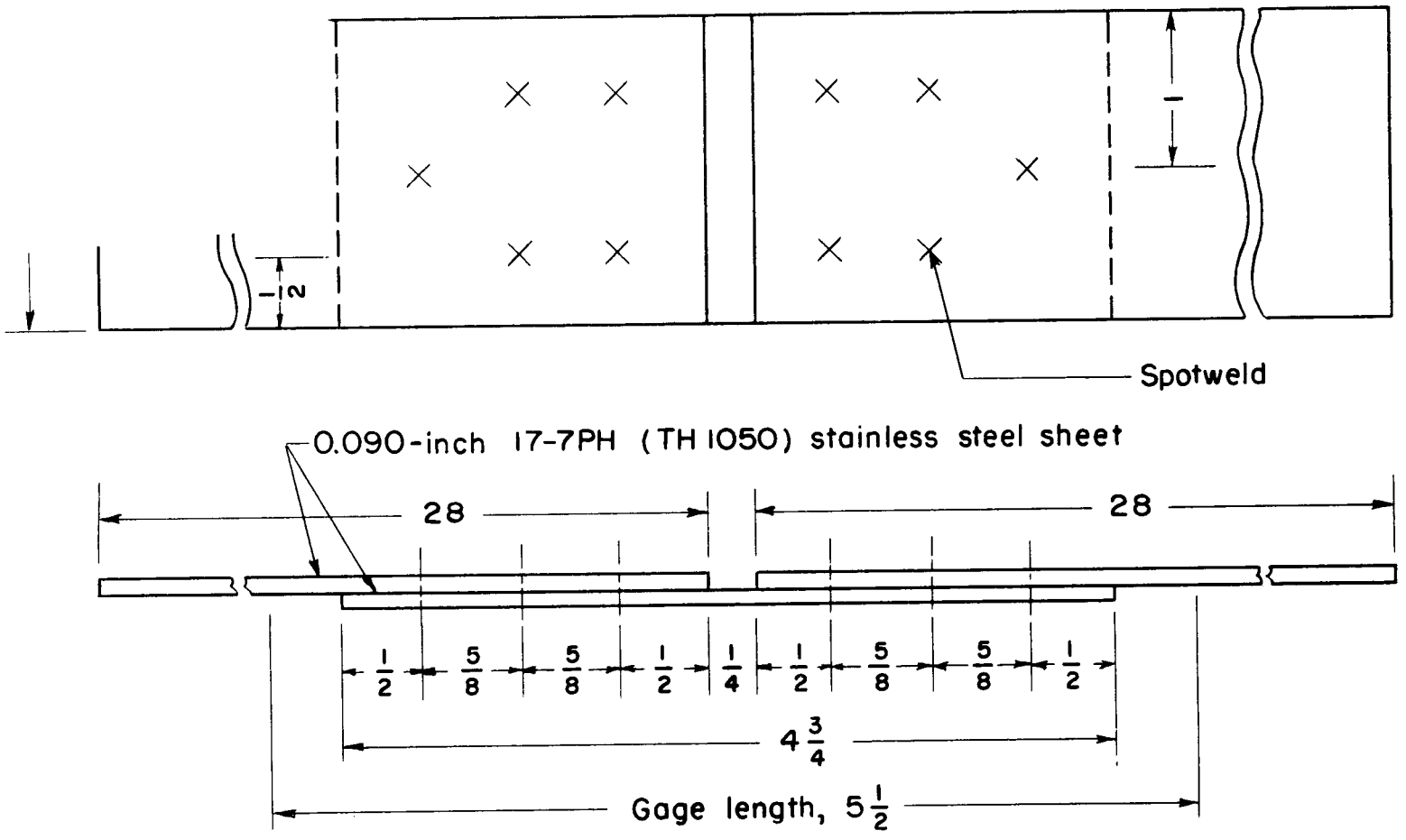


(b) Group Q.

Figure 1.- Continued.

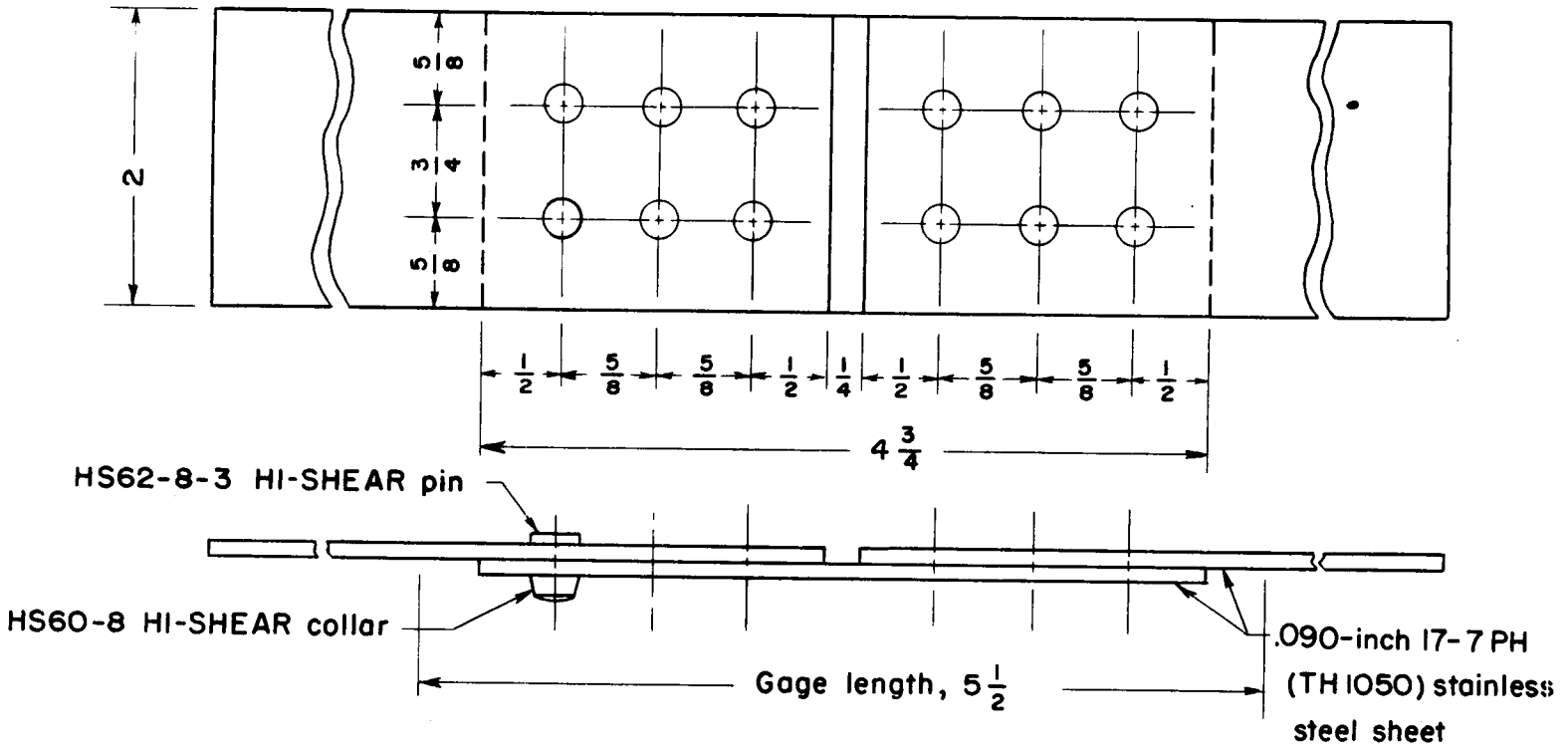


(c) Group R.

Figure 1.- Concluded.

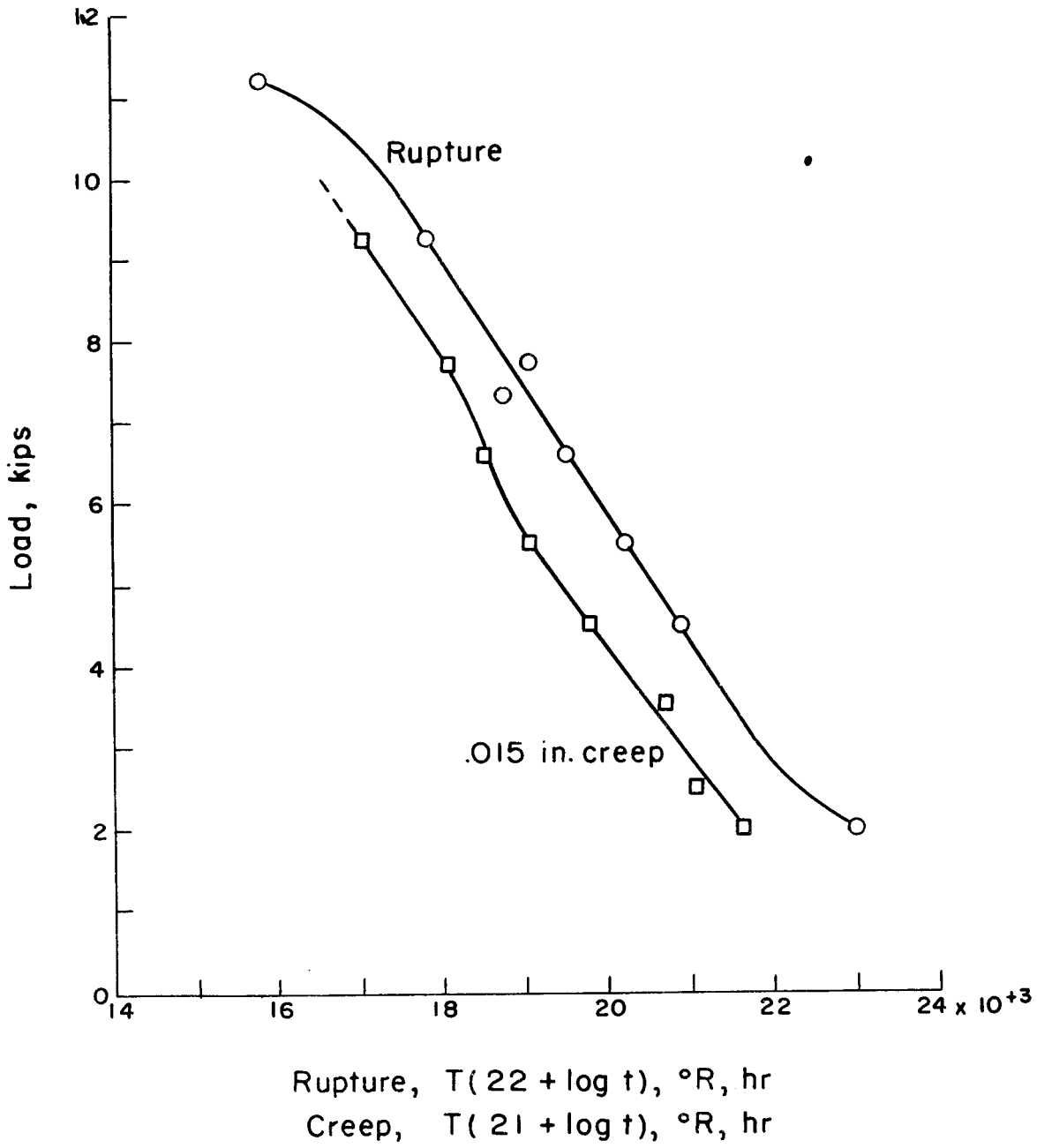


(a) Group D joints.

Figure 2.- Master creep and rupture curves for joints under constant conditions.

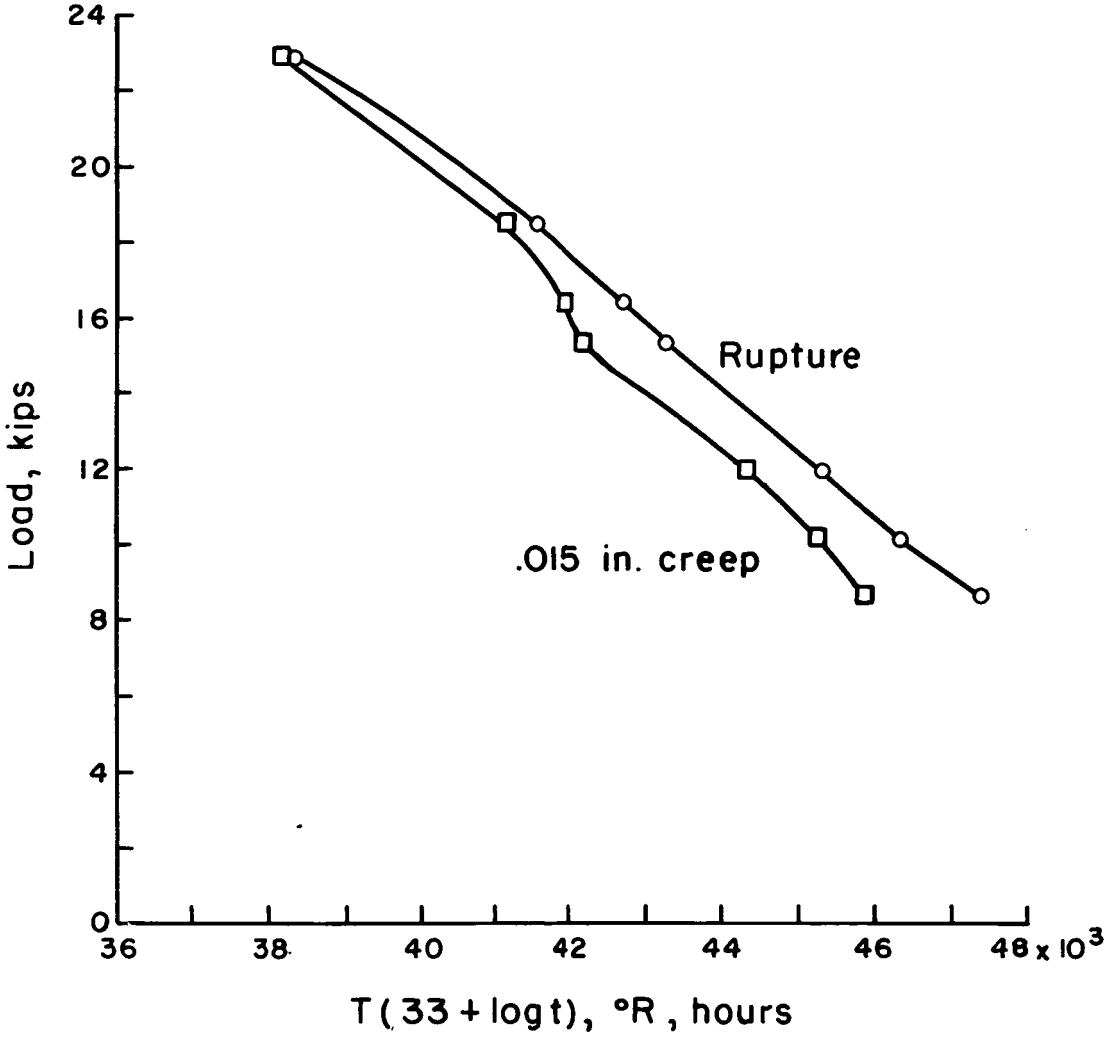


(b) Group Q joints.

Figure 2.- Continued.

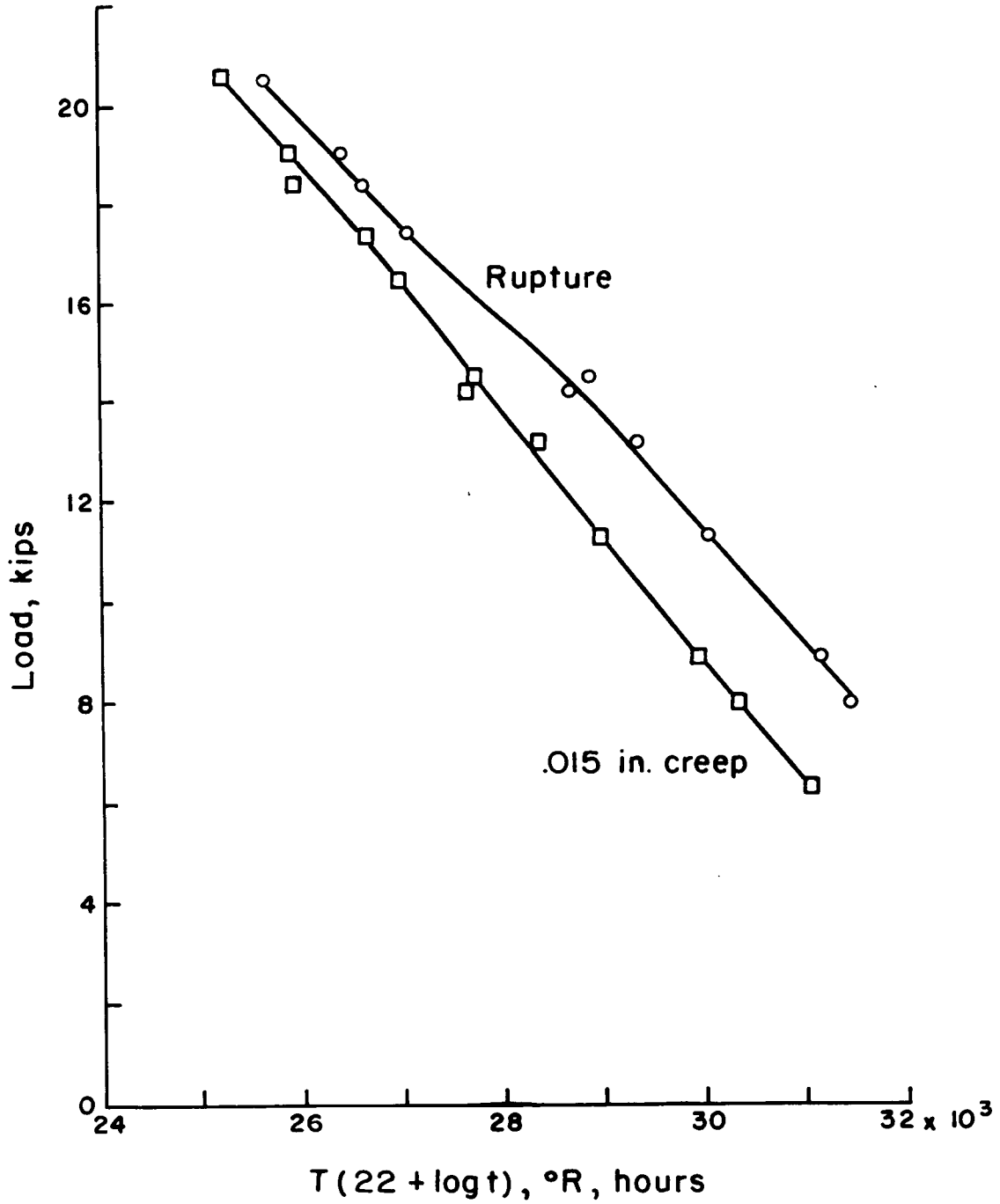


(c) Group R joints.

Figure 2.- Concluded.

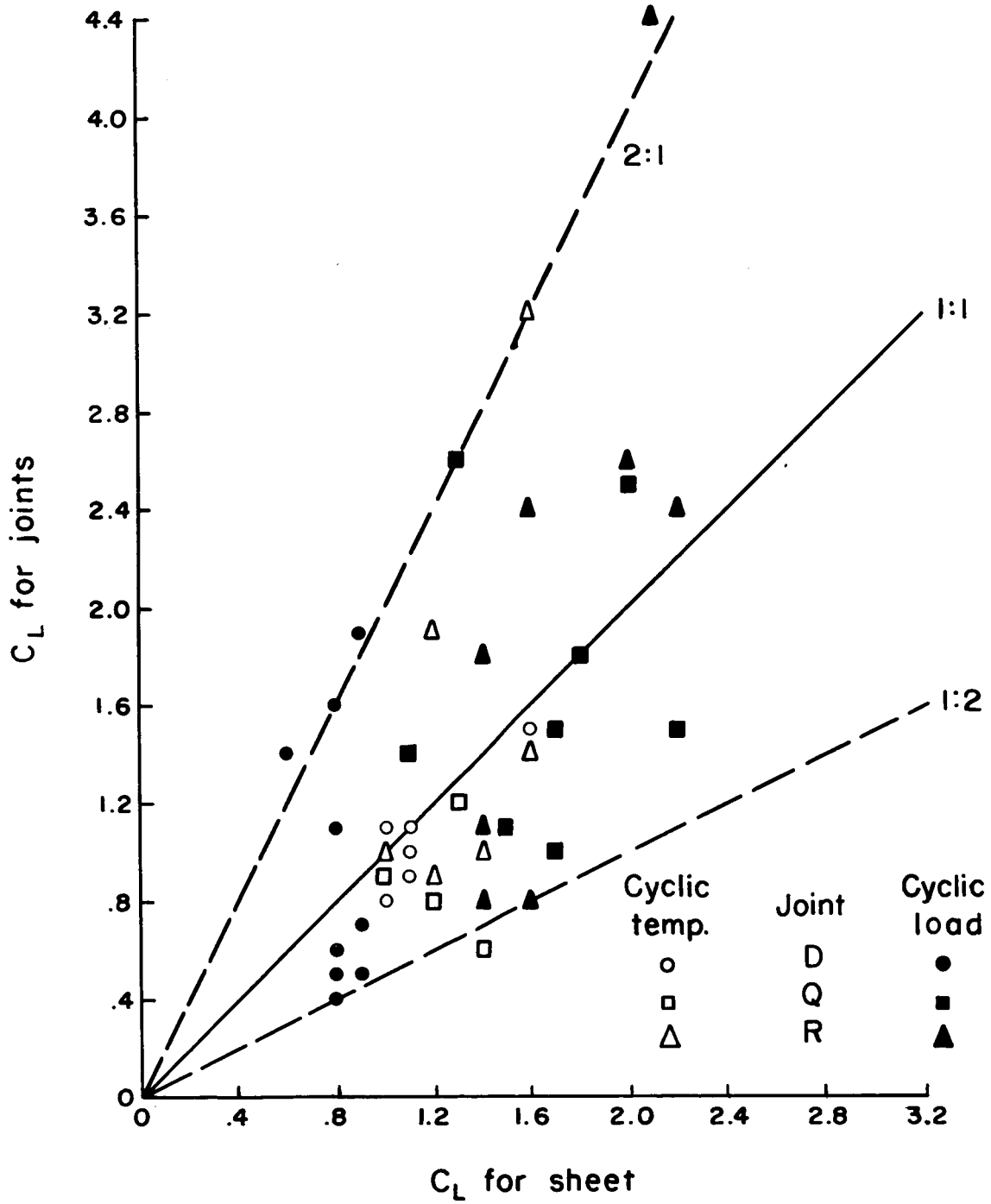


Figure 3.- Comparison of rupture time ratios for joints and sheet material.

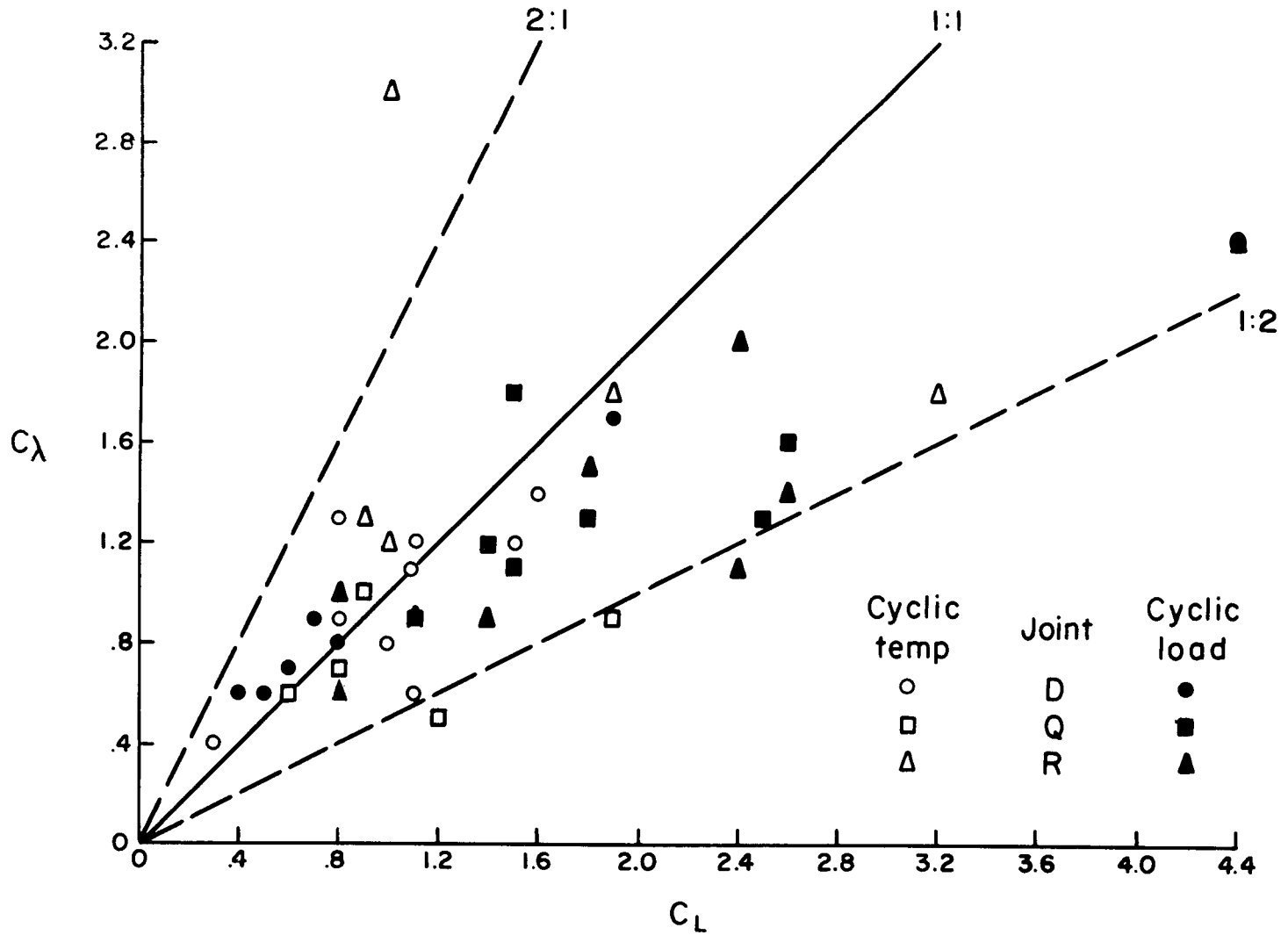


Figure 4.- Comparison of time ratios for deformation and for rupture of joints.

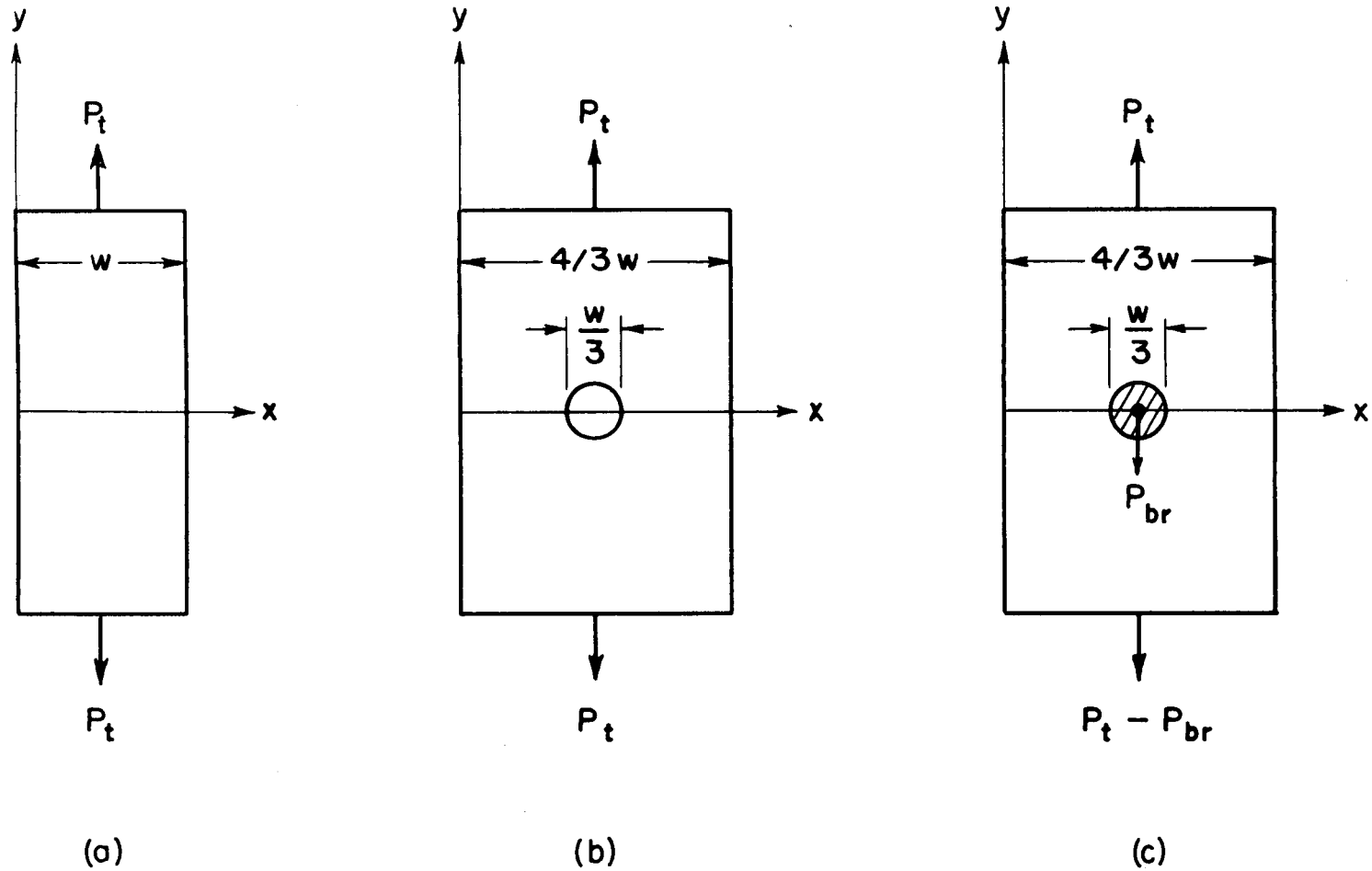


Figure 5.- Schematic representations of specimens: (a) plain sheet in tension, (b) perforated sheet in tension, (c) perforated sheet in tension and bearing.

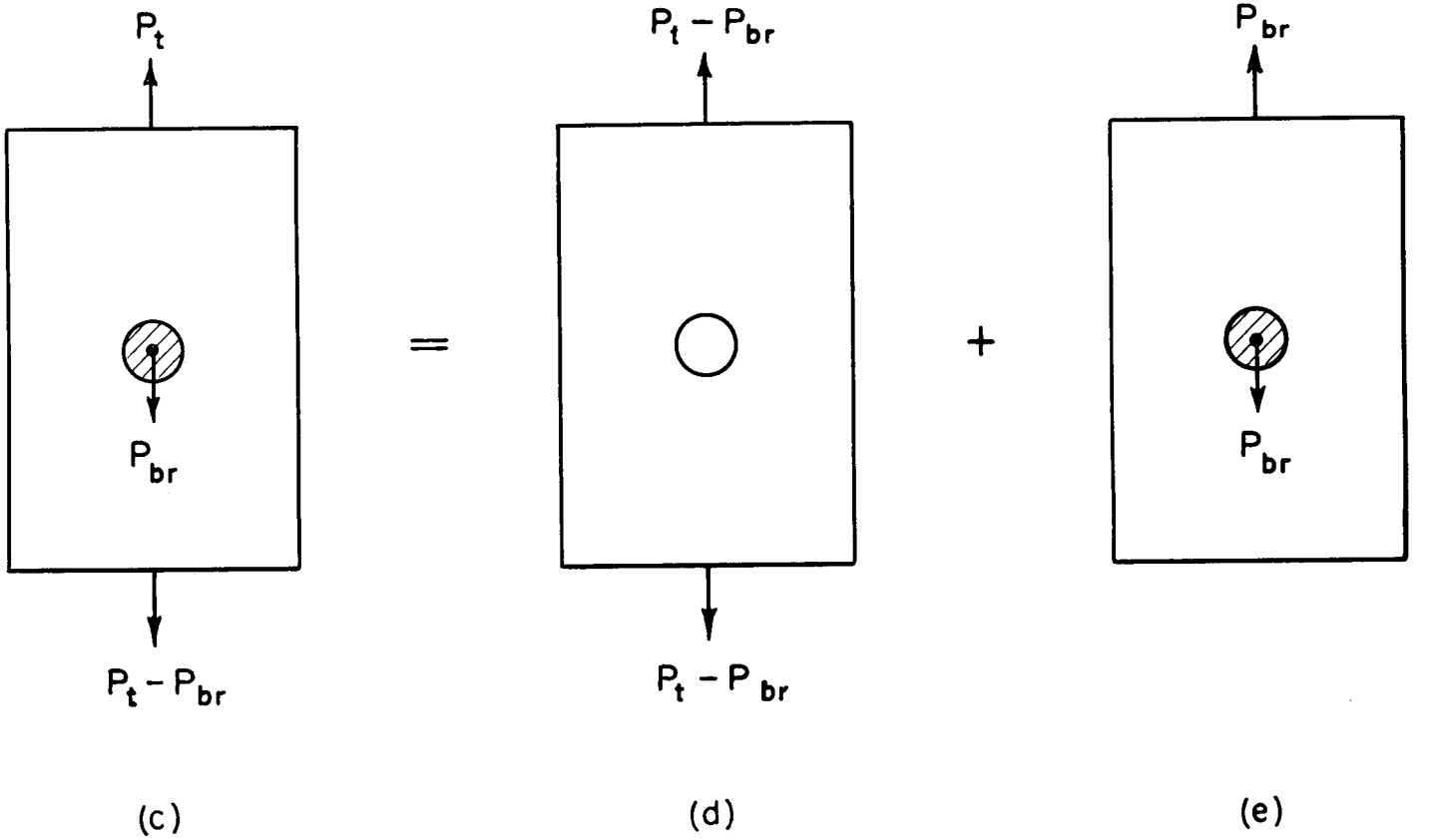


Figure 6.- Schematic representation of superposition: perforated sheet in (c) tension and bearing, (d) tension, (e) bearing.

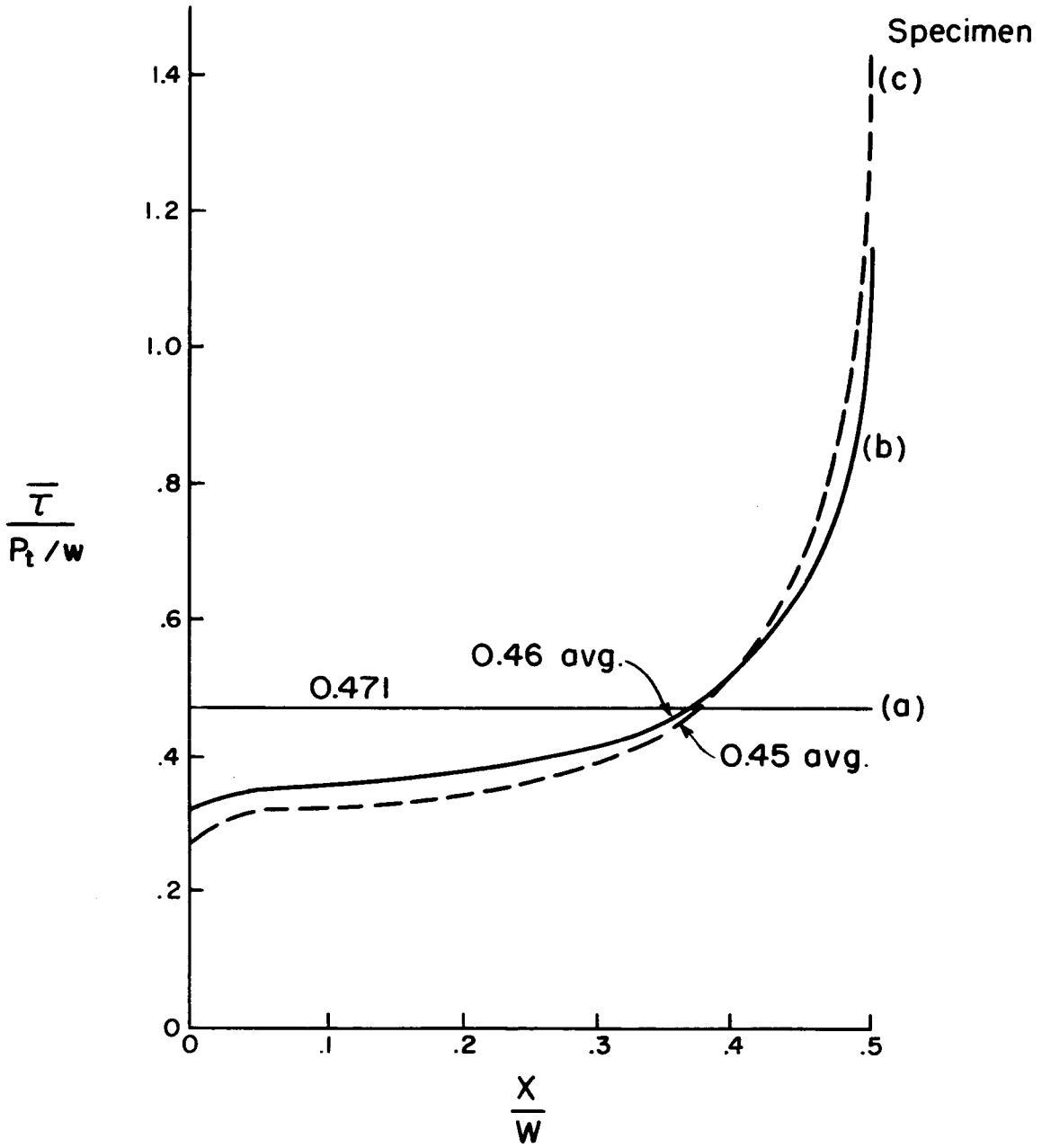


Figure 7.- Distributions and averages of octahedral shear stresses on minimum cross sections of specimens (a), (b), and (c), in figure 5.

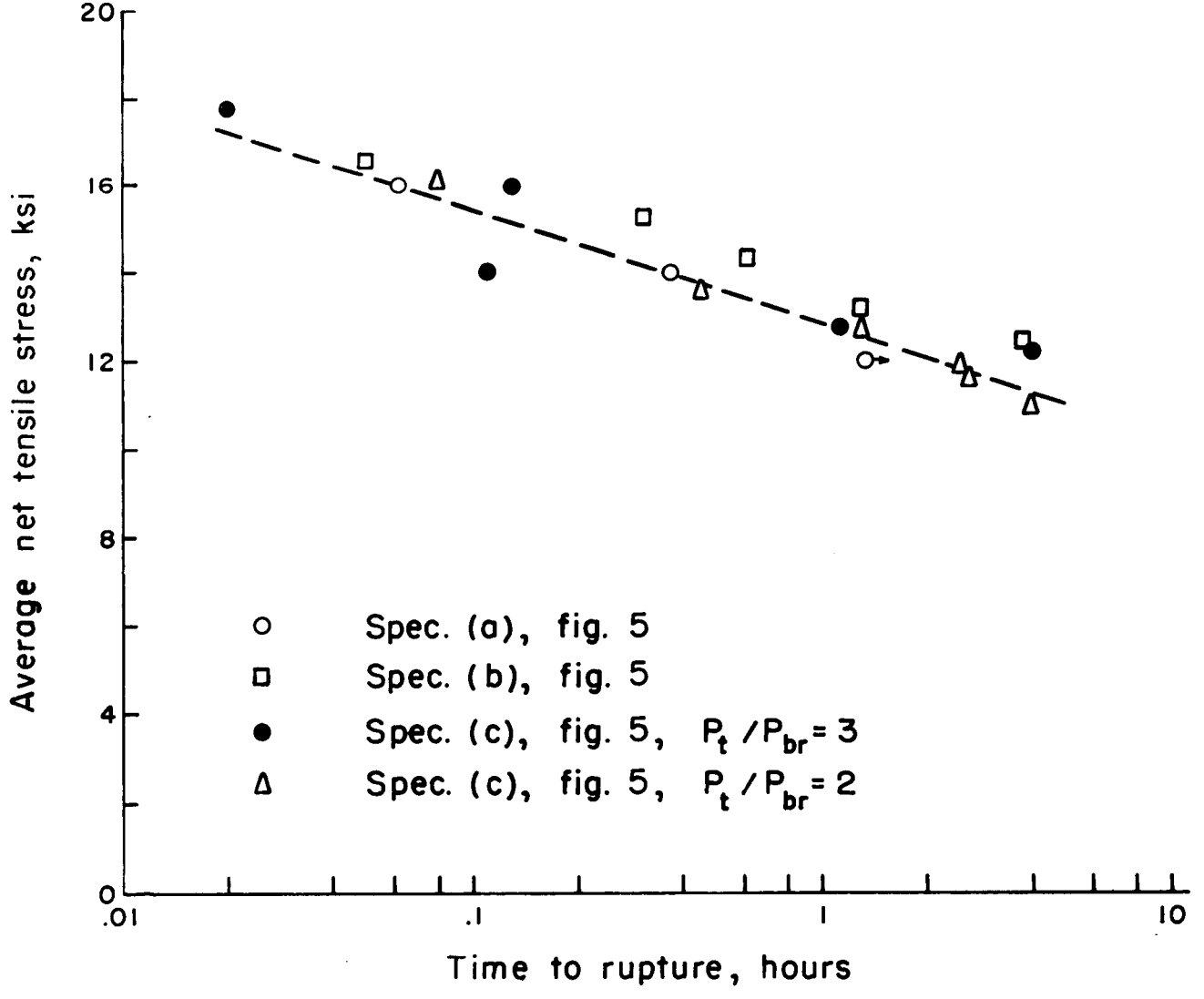


Figure 8.- Effect of bearing on tensile rupture for 2024-0 aluminum alloy at 400° F.

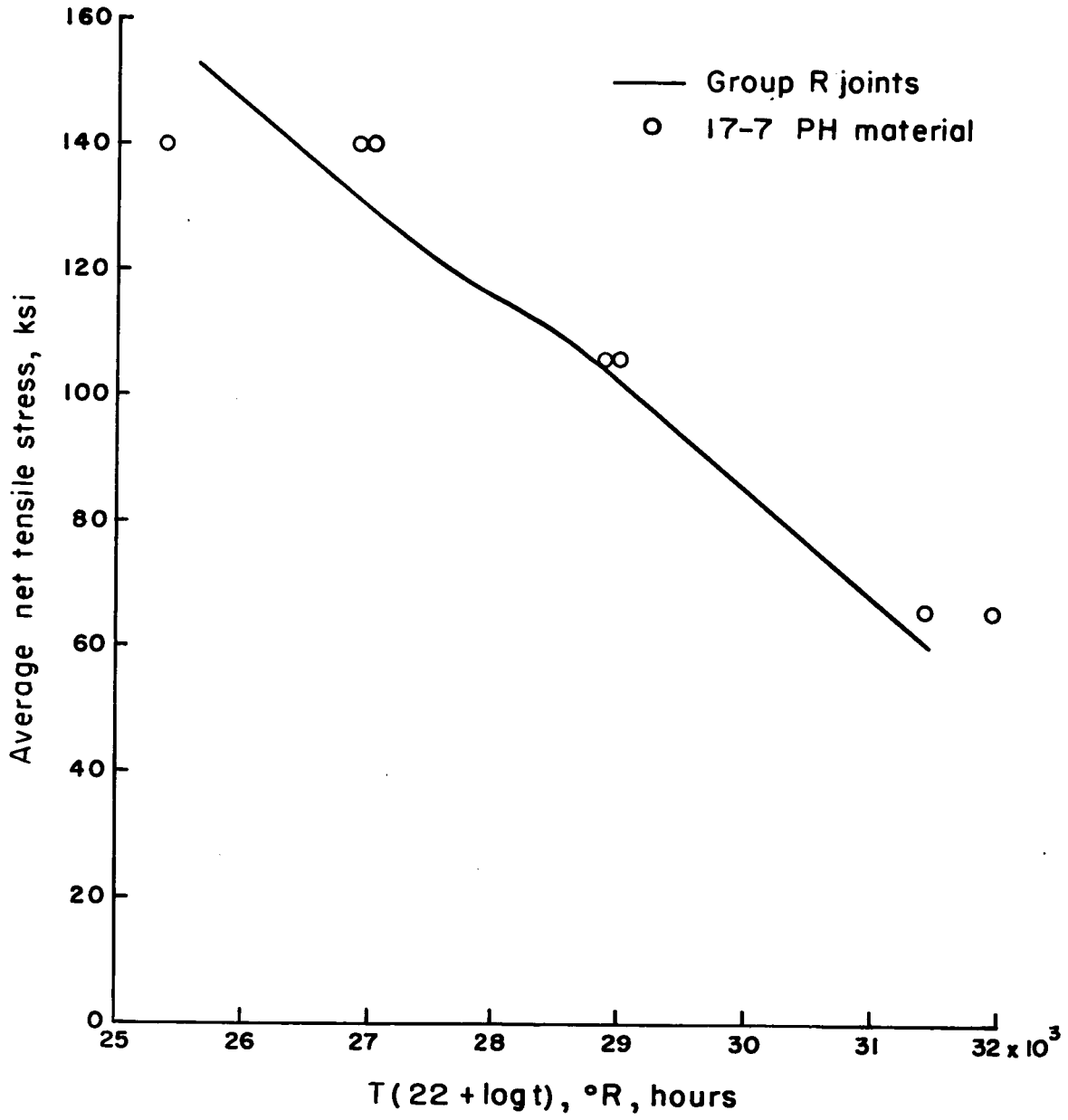


Figure 9.- Comparison of rupture properties of group R joints and 17-7 PH (TH 1050) stainless steel sheet.

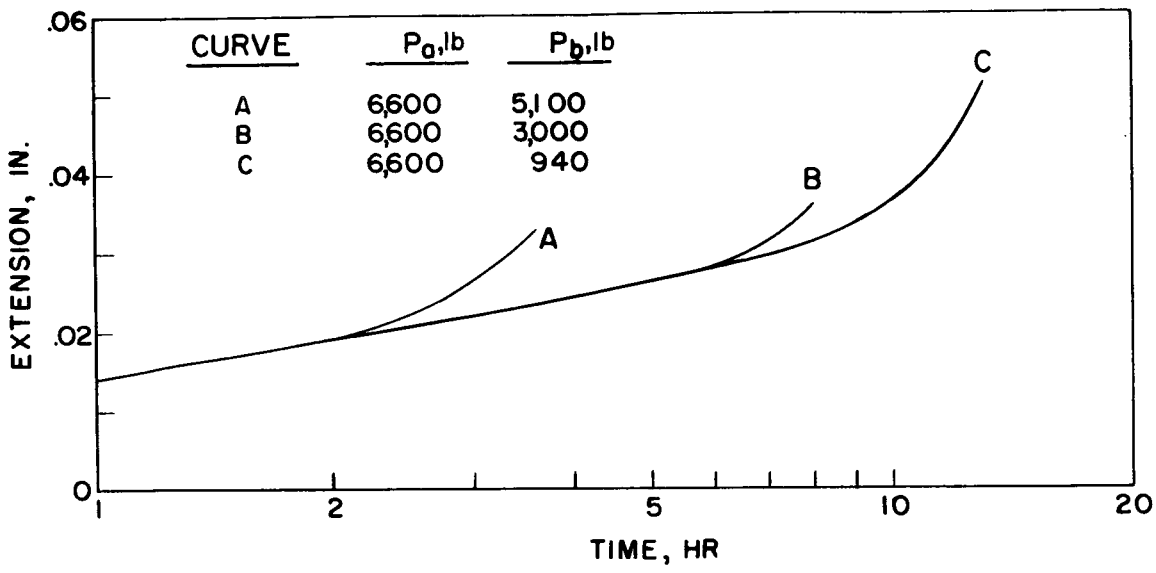


(a) Cyclic load: temperature 400° F, cycle period p = 2 hr.

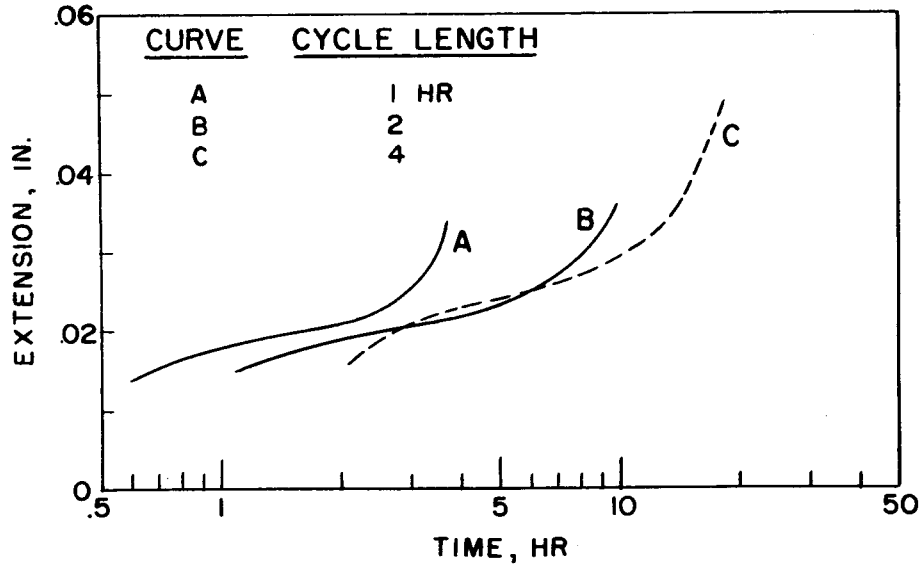


(b) Cyclic temperature: $T_a$ = 400° F, $T_b$ = 75° F, load = 6,600 lb.

Figure 10.- Creep curves of group D joints for cyclic tests at cycle fraction A = 0.5.

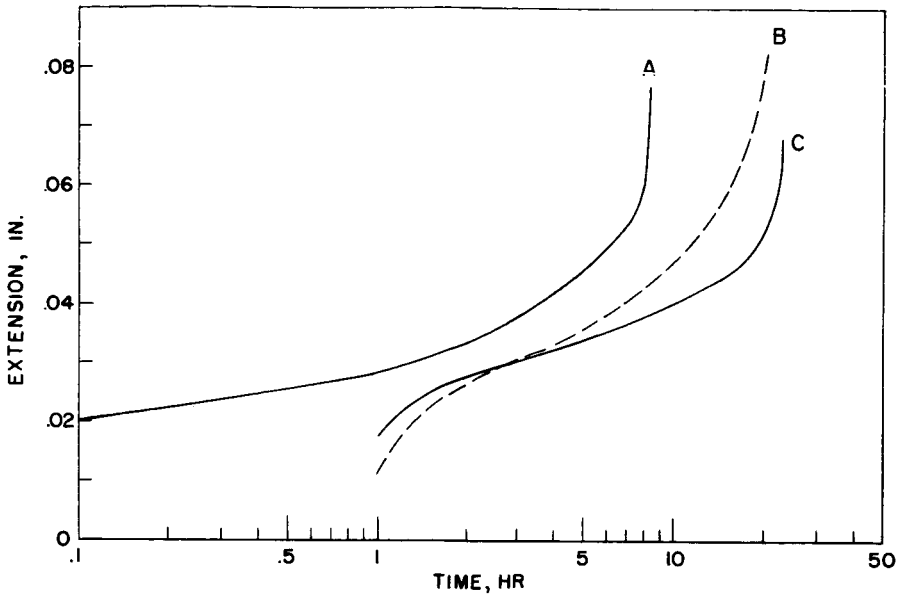


(a) Group Q joints. Curve A: constant temperature, 800° F; constant load, 16,400 lb. Curve B: cyclic temperature, $T_a$ = 800° F, $T_b$ = 75° F; constant load, 16,400 lb. Curve C: constant temperature, 800° F; cyclic load, $P_a$ = 16,400 lb, $P_b$ = 1,000 lb.

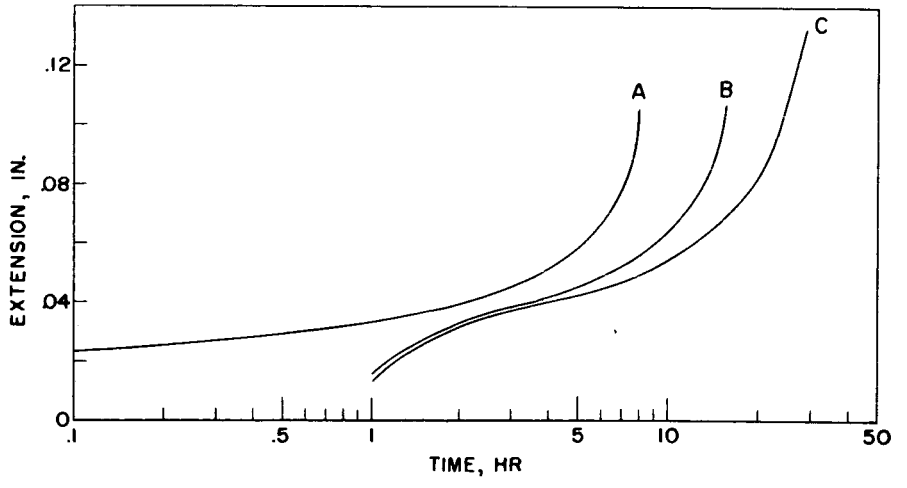


(b) Group R joints. Curve A: constant temperature, 900° F; constant load, 8,900 lb. Curve B: constant temperature, 900° F; cyclic load, $P_a$ = 8,900 lb, $P_b$ = 1,000 lb. Curve C: cyclic temperature, $T_a$ = 900° F, $T_b$ = 75° F; constant load, 8,900 lb.

Figure 11.- Creep curves of group Q and R joints for cyclic tests at cycle fraction A = 0.5 and cycle period p = 2 hr.

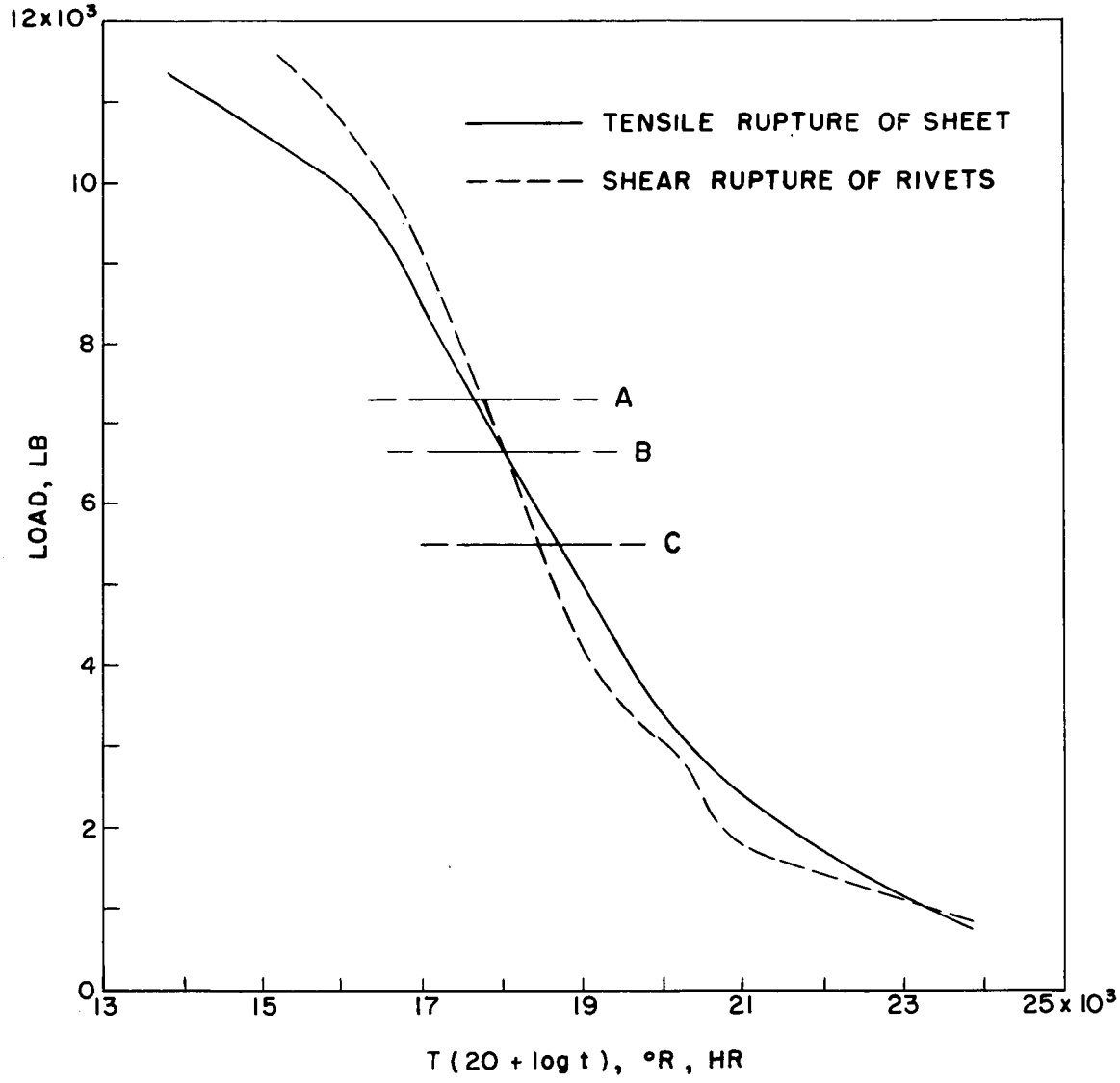


Figure 12.- Calculated master rupture curves for group D joints.

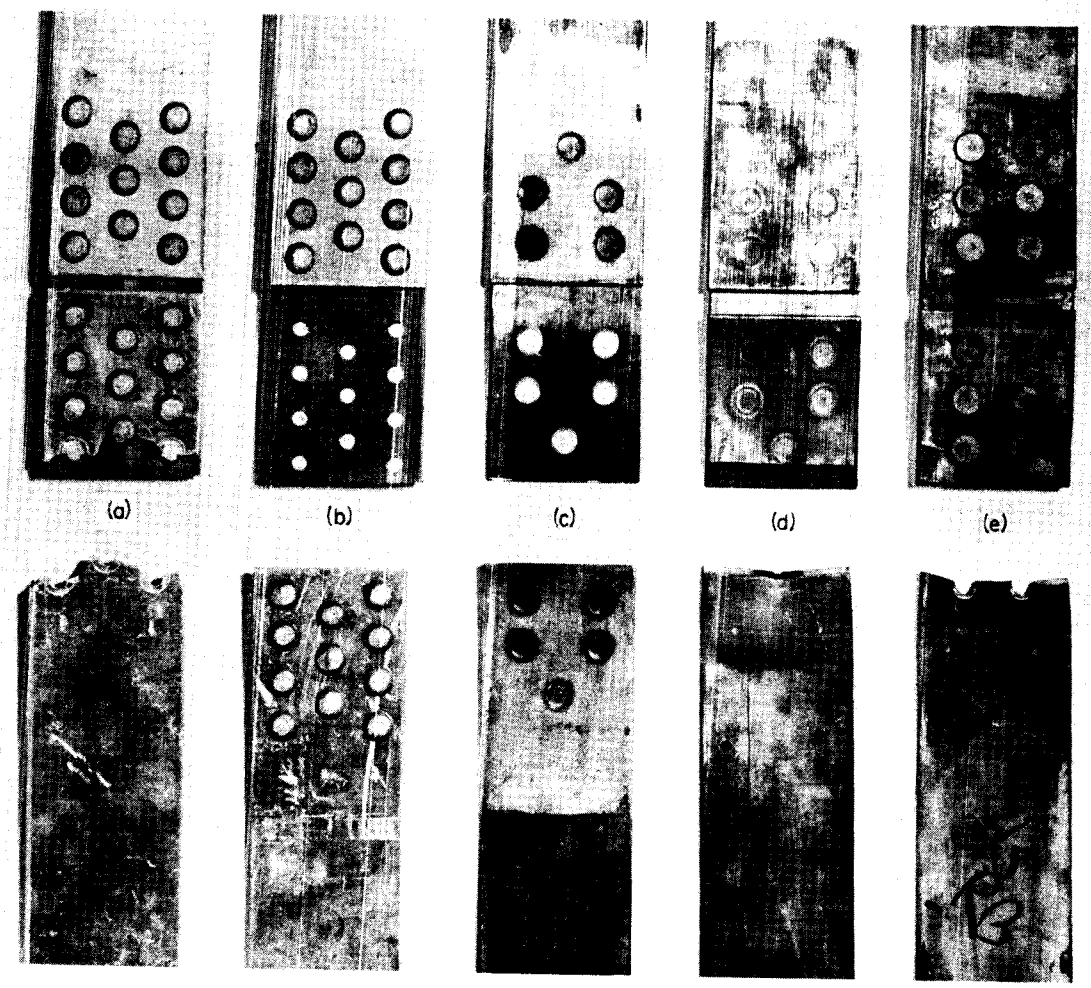


L-59-3072

Figure 13.- Typical failures of joint specimens. Left to right: (a) tensile failure of group D joint; (b) shear failure of group D joint; (c) shear failure of group Q joint; (d) tensile failure of group Q joint; (e) tensile failure of group R joint.